

Development of InGaAs photodiodes for near-infrared spectroscopy

Non-member	Morio Wada	(Yokogawa Electric Co.)
Non-member	Shoujiro Araki	(Yokogawa Electric Co.)
Non-member	Takahiro Kudou	(Yokogawa Electric Co.)
Non-member	Toshimasa Umezawa	(Yokogawa Electric Co.)
Non-member	Shinichi Nakajima	(Yokogawa Electric Co.)
Member	Toshitsugu Ueda	(Yokogawa Electric Co.)

Lattice-mismatched InGaAs photodiodes with low dark current and very wide wavelength spectral response for near-infrared spectroscopy applications are presented. We have demonstrated almost complete relaxation of the strain by using the composition-graded InAsP buffer and also shown good reproducibility of the PD fabrication process.

Keywords: lattice mismatch, photodiodes, InGaAs, near-infrared spectroscopy

1. Introduction

Near-infrared spectrometry is being applied to quality/process control in many industrial areas such as petrochemicals, foodstuffs, beverages and pharmaceuticals, and is expected to offer a spectroscopic solution for non-invasive measurement in medical research and in environmental monitoring and imaging of gases and temperature. Lattice-mismatched InGaAs photodiodes (PDs) have been widely studied as highly sensitive extended-wavelength photodetectors in the near infrared region from 0.8 to 2.5 μm ⁽¹⁾⁻⁽⁷⁾. However, several problems limit the applicability of this approach. For example, the strain between an InGaAs light-absorbing layer and an InP substrate is not completely relaxed in the buffer layer, and hence the strain affects the determination of composition. In most cases, it was found that a relatively high dark current and the poor reproducibility of the InGaAs composition limited the effectiveness of this approach ⁽⁷⁾. In addition, lower quantum efficiency at the shorter wavelengths is due to the strong light absorption of the thick cap layer ⁽⁴⁾.

In this paper we show that, using a very thin InAsP cap layer and composition-graded InAsP buffer, one can solve most of these problems and fabricate good quality lattice-mismatched InGaAs PDs with good reproducibility for detection over the entire near-infrared wavelength region.

2. Device Structure and Fabrication

The cross section of the PD epitaxial wafer structure is shown in Fig. 1. InP, InAsP and InGaAs were grown on (100) InP substrates misoriented 2° toward <110> by metalorganic vapor-phase epitaxy (MOVPE) using an AIXTRON AIX 200/4 system. First, an S-doped, composition-graded *n*-InAsP buffer was grown, followed by growth of the *n*-In_{0.80}Ga_{0.20}As light-absorbing layer. The composition-graded InAsP buffer consists of fifteen steps of InAs_yP_{1-y} (*y*=0-0.63) and a 2- μm thick InAs_{0.63}P_{0.37} layer. The thickness of the InAs_{0.63}P_{0.37} cap layer is as thin as 200 nm to reduce the light absorption of the cap layer at the shorter

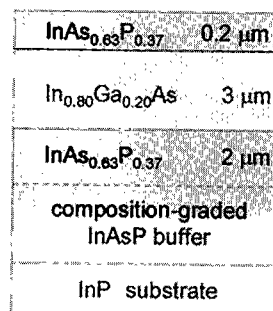


Fig. 1 Schematic cross section of PD epitaxial wafer structure.

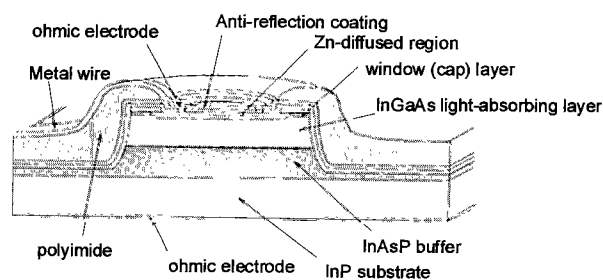


Fig. 2 Schematic of PD with thin window (cap) layer and InAsP buffer.

wavelength. The lattice mismatch of In_{0.80}Ga_{0.20}As and InAs_{0.63}P_{0.37} to InP is +2.0%.

Figure 2 is a schematic cross section of the lattice-mismatched InGaAs photodiode. Selective Zn diffusion was carried out by the metalorganic vapor-phase diffusion (MOVPE) technique and the diffusion depth was 200 nm from the interface between the InAs_{0.63}P_{0.37} cap and In_{0.80}Ga_{0.20}As light-absorbing layers. Photolithography and chemical etching was followed by deposition of SiO₂/Si₃N₄ films as an antireflection coating and the formation of ohmic contact electrode defined mesas. The photosensitive area of the PD was 1 mm in diameter.

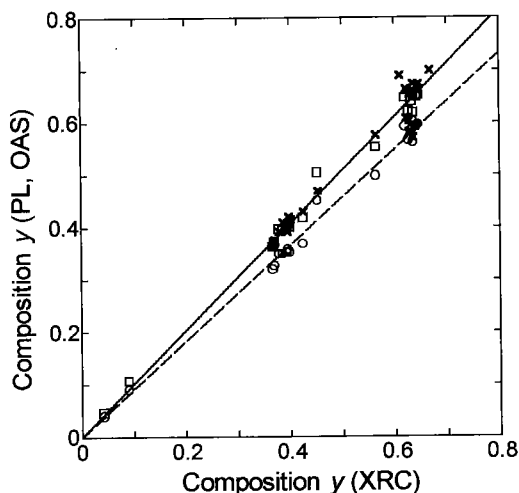


Fig. 3 Comparison of the composition y of $\text{InAs}_y\text{P}_{1-y}$ obtained from XRC to that from PL and OAS. The compositions calculated from PL data by Eq. (1) and the equation reported by Antipas *et al.* are represented by symbols \square and \circ , respectively. The values obtained from OAS measurements are represented by \times . Solid and dashed lines were computed using a least squares program.

To precisely determine the alloy composition and strain relaxation for the InAsP buffer, X-ray rocking curves (XRC), photoluminescence (PL) and optical absorption spectra (OAS) were measured. For $\text{InAs}_y\text{P}_{1-y}$, the variation of the band gap with As composition y was not well established. The alloy composition of $\text{InAs}_y\text{P}_{1-y}$ from PL and OAS was calculated by the empirical equation that we have proposed:

$$E_g = 1.407 - 1.073y + 0.089y^2 \dots \dots \dots (1)$$

Here E_g is the band gap energy of $\text{InAs}_y\text{P}_{1-y}$ with no strain at 77 K⁽⁶⁾. The $\text{InAs}_y\text{P}_{1-y}$ epitaxial layers prepared for this study were also grown on the composition-graded InAsP buffer layer to relax the strain induced by the lattice-mismatch of

$\text{InAs}_y\text{P}_{1-y}$ to InP substrates. Figure 3 shows the composition y of $\text{InAs}_y\text{P}_{1-y}$ obtained from PL, OSA and XRC. The lattice constant for unstrained $\text{InAs}_y\text{P}_{1-y}$ is known to vary linearly with composition and the relation between the composition y and the lattice constant a can be expressed as

$$a(y) = 0.1894y + 5.8696 \dots \dots \dots (2)$$

In the case of unstrained layers, $a = a_{\perp} = a_{\parallel}$ where a_{\perp} and a_{\parallel} are the lattice parameters of the unit cells perpendicular and parallel to the interface between the layer and the substrate, respectively. XRC was carried out in the (400) reflection mode with $\text{Cu K}\alpha_1$ ($\lambda_{\text{CuK}\alpha_1} = 0.15056 \text{ nm}$) beam. From the Bragg relation $\lambda_{\text{CuK}\alpha_1} = 2a \sin \theta$, the fractional difference in lattice parameter is given by

$$\frac{\Delta d}{d} = -\Delta \theta \cot \theta = \frac{a_s - a}{a_s} \dots \dots \dots (3)$$

where θ is a Bragg angle with respect to the InP substrate

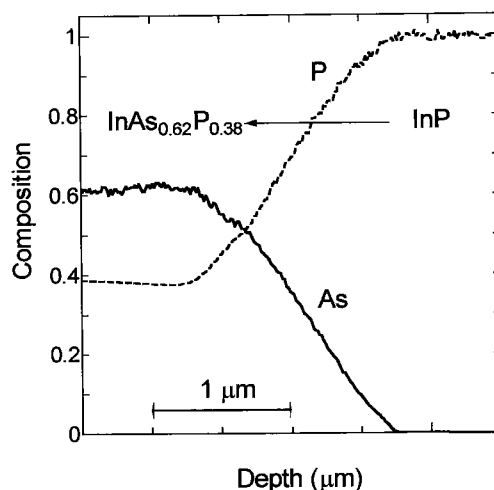


Fig. 4 In-depth profiles for the compositions of As and P in the linear-composition-graded InAsP buffer obtained by SIMS analysis.

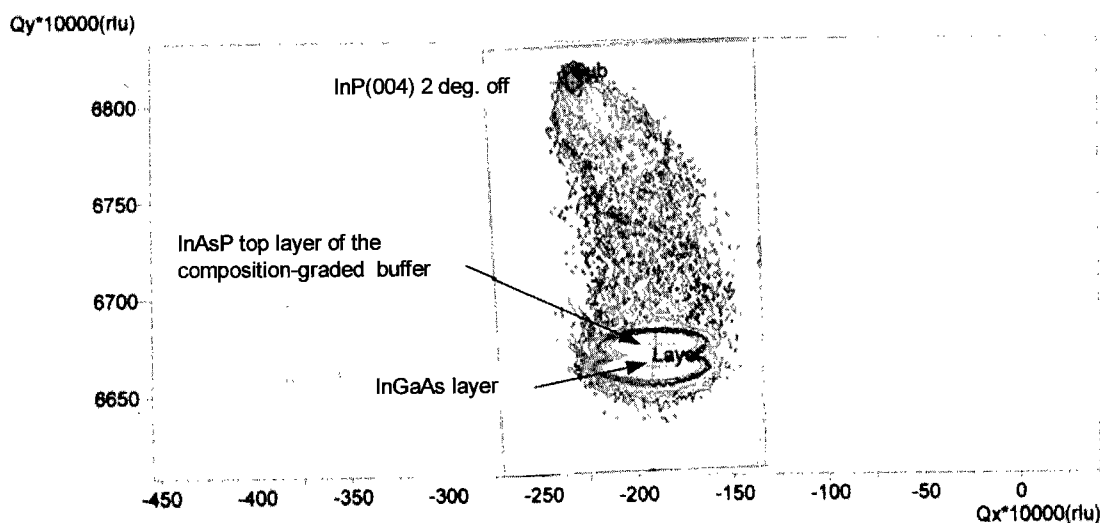


Fig. 5 (004) reciprocal space map for the epitaxial wafer in Fig. 1.

(100) plane and $\Delta\theta$ is measured directly by the peak separation in the (400) X-ray diffraction curve.

The compositions obtained from XRC agree well with the values calculated by Eq. (1). In Fig. 3 the dashed line shows the calculation carried out using the equation given by Antypas and Yep⁽⁹⁾, which has been widely used for band gap calculation of InGaAsP quaternary alloy with no strain^{(10), (11)}.

We designed the linear-composition-graded InAsP buffer. The top layer of the buffer was as thick as 2 μm , as shown in Fig. 1, and its composition was determined by using PL, OAS and XRC measurements. Figure 4 shows the in-depth SIMS profiles for the composition-graded InAsP buffer where the atomic compositions for As and P are calculated from the intensities of As and P signals. In MOVPE growth, the growth rate for $\text{InAs}_y\text{P}_{1-y}$ is subject to In mole fraction regardless of the flow rates of the group V sources, resulting in the constant growth rate of $\text{InAs}_y\text{P}_{1-y}$ during the growth of the composition-graded buffer.

The (004) and (204) X-ray diffraction reciprocal-lattice space maps for the epitaxial wafer in Fig. 1 were measured by high-resolution X-ray diffraction using a Philips X'Pert diffractometer. Figure 5 shows the result for the (004) diffraction space maps in units of $1/\text{rlu} = \lambda_{\text{CuK}\alpha} / 2d$, where d is the lattice parameter in the given directions. The three main peaks are from the InP substrate, the thick top layer of the composition-graded InAsP buffer and the InGaAs light-absorbing layer. The strain is relaxed in the composition-graded InAsP buffer, and the InGaAs light-absorbing layer is lattice-matched to the thick top layer of the buffer, as seen in Fig. 5. By measuring the relative positions of the diffraction peaks from the layers and substrate, we determined the lattice parameters of the unit cells for the top layer of the composition-graded buffer and the InGaAs light-absorbing layer⁽¹²⁾. The percentage relaxation R is given by

$$R = (a_{\parallel} - a_s) / (a_{\perp} - a_s) \times 100 (\%) \quad (4)$$

Here a_s is the lattice parameter of the substrate and $a_s =$

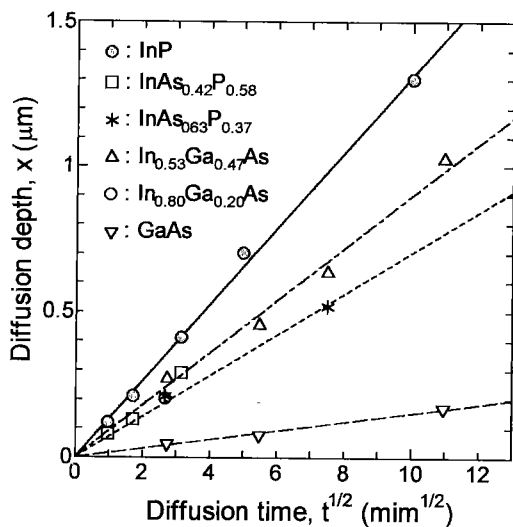


Fig. 6 Comparison of diffusion depth for InP, InAsP, InGaAs and GaAs.

0.58696 nm for InP. This definition of R gives $R=0\%$ when no misfit dislocations are presented and $R=100\%$ when the layer unit cell has cubic symmetry. For the InAsP top layer, the lattice parameters a_{\perp} and a_{\parallel} were measured to be 0.5994 and 0.5992 nm, respectively. R is calculated to be 98.4% for the InAsP top layer, resulting that the layer unit cell is nearly cubic symmetry then the InAsP top layer on the composition-graded InAsP buffer is almost fully relaxed.

The lattice mismatches of the InGaAs light-absorbing layer to the InAsP top layer with respect to the lattice parameters a_{\perp} and a_{\parallel} were calculated to be 1.67×10^{-3} and -8.34×10^{-4} , respectively.

A new technique of Zn diffusion, MOVPD, that we have developed was applied to the formation of a shallow pn junction through a very thin InAsP cap layer^{(13), (14)}. Compared to the previous Zn diffusions such as closed-ampoule diffusion and diffusion from spin-on glass, significantly lower Zn diffusivity can be realized by MOVPD. Figure 6 shows a plot of diffusion depth versus the square root of diffusion time for InP, InAsP and InGaAs under the specified diffusion conditions. The values for GaAs are the data reported by Paska *et al*⁽¹⁵⁾. It was found that the difference of Zn diffusivity between $\text{InAs}_{0.63}\text{P}_{0.37}$ and $\text{In}_{0.80}\text{Ga}_{0.20}\text{As}$ was very small, thus simplifying control of the Zn diffusion depth to form a shallow pn junction. The Zn diffusion profile obtained by SIMS analysis is shown in Fig. 7. The diffusion depth is approximately 200 nm from the heterointerface between the InAsP cap and InGaAs light-absorbing layer. Zn doping as high as $2 \times 10^{19} \text{ cm}^{-3}$ is achieved for the $\text{InAs}_{0.63}\text{P}_{0.37}$ cap layer, so the cap layer also can act as a good ohmic contact layer.

3. Device Characteristics

Figure 8 shows the reverse current versus voltage characteristics for the twenty PDs measured at $294 \pm 1 \text{ K}$. The dark current at a reverse applied voltage of 10 mV is 5 μA . The shunt resistance, which is defined as the resistance when a reverse voltage of 10 mV is applied, is 2 $\text{K}\Omega$. The thermal activation energy for the dark current was measured

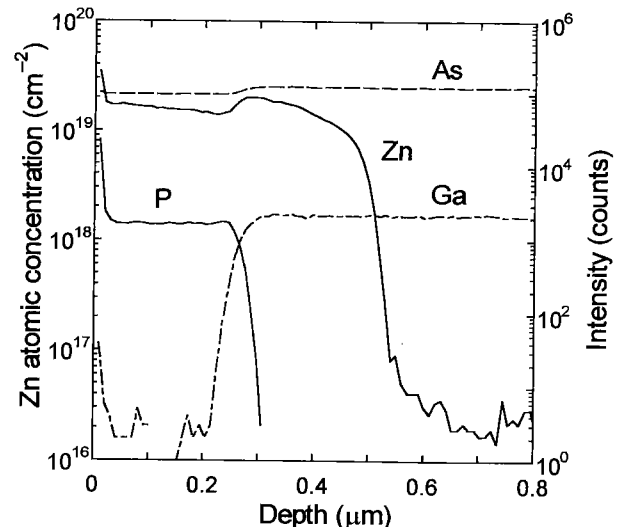


Fig.7 Profiles of Zn concentration and ion intensities of As, Ga and P obtained by SIMS analysis.

to be 0.45 eV in the temperature range from 233 to 313 K.

Figure 9 shows the responsivity of the PD measured at 294 ± 1 K in the near-infrared wavelength region compared to the responsivity of conventional Si, lattice-matched InGaAs and extended-wavelength InGaAs *pin* PDs. The dashed lines in Fig. 9 represent the calculations with theoretical quantum efficiencies of 60, 70 and 80%. The results show that the new PD in this study can be not only operated in a wavelength range much wider than that of conventional PDs, but also have responsivity as high as that of conventional PDs.

From these results the noise equivalent power for the peak wavelength λ_p of 2-2.3 μm was calculated to be $1.3 \pm 0.05 \times 10^{-12}$ and $3.2 \pm 0.1 \times 10^{-12}$ W/Hz^{1/2} at 294 and 253 K, respectively. These values are the lowest achieved to date for lattice-mismatched InGaAs PDs realized by both hydride vapor-phase epitaxy and MOVPE.

In order to use the devices at an environment temperature of around 300 K, the PD chips were mounted on an electric cooler and were hermetically packaged in a metal package with a glass window, as shown in Fig. 10. At an environment temperature of 294 ± 1 K, the temperature of the PD chip could be controlled from 258 K to room temperature with

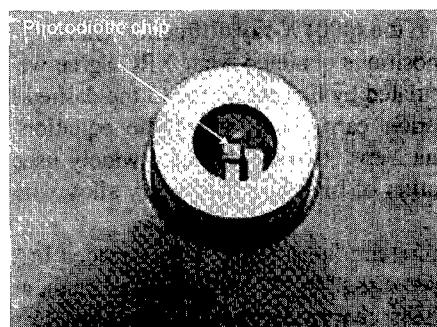


Fig. 10 Photograph of the PD packaged with a thermoelectric cooler.

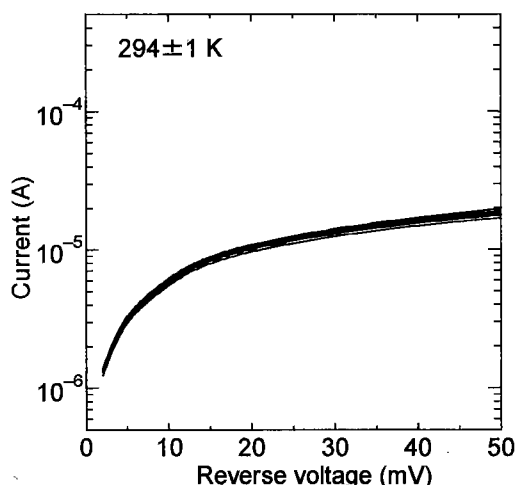


Fig. 8 Reverse current versus voltage characteristics for the twenty PDs measured at 294 ± 1 K.

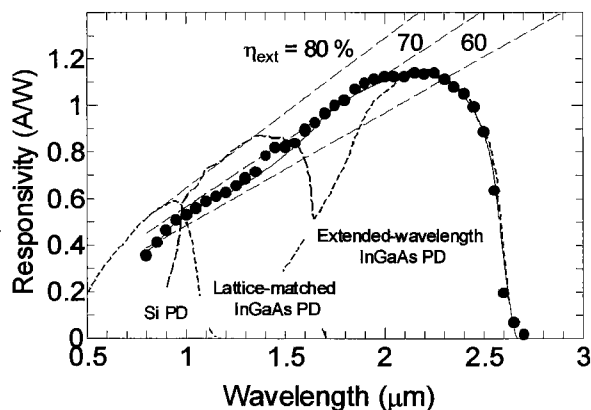


Fig. 9 Measured responsivity of the PD and comparison to responsivities of conventional Si, lattice-matched InGaAs and extended-wavelength InGaAs *pin* PDs.

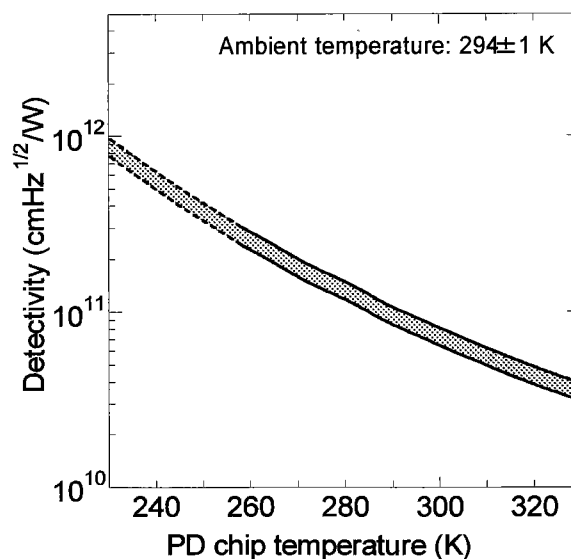


Fig. 11 Detectivity of the packaged PD as a function of PD chip temperature at an ambient temperature of 294 ± 1 K.

high temperature stability, and the detectivity D^* of 1 to 3×10^{11} cmHz^{1/2}/W for $\lambda_p = 2.0\text{-}2.3$ μm was obtained as shown in Fig. 11.

4. Conclusion

We have demonstrated a very wide wavelength range of 0.8-2.5 μm and a high detectivity of 10^{11} cmHz^{1/2}/W at peak wavelengths of 2-2.3 μm at room temperature for lattice-mismatched InGaAs *pin* PDs based on a design with a very thin cap layer and a composition-graded buffer. We have demonstrated almost complete relaxation of the strain by using the composition-graded InAsP buffer and also shown good reproducibility of the PD fabrication process.

Acknowledgments

The authors would like to thank M. Toyonori for his continuous support and encouragement for this work. Sincere thanks are due also to Dr. K. Saito and K. Hirose of Philips Japan, Ltd. for the use of their X-ray analyzer and for the measurements. This work was partly supported by the

R&D Institute for Photonics Engineering, the Manufacturing Science and Technology Center, and the New Energy and Industrial Technology Development Organization.

(Manuscript received May 31, 2001, revised Aug. 2, 2001)

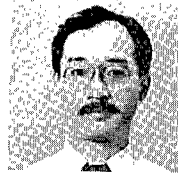
References

- (1) R. R. Saxena, S. B. Hyder, P. E. Gregory and J. S. Escher, Vapor phase epitaxial growth of InGaAs/InAsP heterojunctions for long wavelength transferred electron photocathodes, *J. Crystal Growth* 50, pp. 481-484, 1980.
- (2) K. Makita, T. Torikai, H. Ishihara and K. Taguchi, $Ga_{1-y}In_yAs/InAs_xP_{1-x}$ ($y>0.53$, $x>0$) pin photodiodes for long wavelength regions ($\lambda>2$ mm) grown by hydride vapor phase epitaxy, *Electron. Lett.* 24, pp. 379-380, 1988.
- (3) R. U. Martinelli, T. J. Zamerowski and P. A. Longeway, 2.6 μm InGaAs photodiodes, *Appl. Phys. Lett.* 53, pp. 989-991, 1988.
- (4) K. R. Linga, G. H. Olsen, V. S. Ban, A. M. Joshi and W. F. Kosonocky, Dark current analysis and characterization of $In_xGa_{1-x}As/InAs_yP_{1-y}$ graded photodiodes with $x>0.53$ for response to longer wavelengths (>1.7 μm), *J. Lightwave Technol.* 10, pp. 1050-1055, 1992.
- (5) M. A. Di Forte-Poisson, C. Brylinski, Di Persio, J. X. Hugon, B. Vilotecg and C. Le Noble, $In_xGa_{1-x}As/InAs_yP_{1-y}$ photodiodes for the 1.6 to 2.4 μm spectral region grown by low pressure MOVPE, *J. Crystal Growth* 124, pp. 782-791, 1992.
- (6) M. Wada and H. Hosomatsu, Wide wavelength and low dark current lattice-mismatched InGaAs/InAsP photodiodes grown by metalorganic vapor-phase epitaxy, *Appl. Phys. Lett.* 64, pp. 1265-1267, 1994.
- (7) M. D'Hondt, L. Moerman, P. Van Deale and P. Demeester, Influence of buffer layer and processing on the dark current of 2.5 μm -wavelength 2%-mismatched InGaAs photodiodes, *IEE Proc. -Optoelectron.* 144, pp. 277-282, 1997.
- (8) M. Wada, S. Araki, T. Kudou, T. Umezawa, S. Nakajima and T. Ueda, Temperature dependence of the band gap in $InAs_yP_{1-y}$, *Appl. Phys. Lett.* 76, pp. 2722-2724, 2000.
- (9) G. A. Antypas and T. O. Yep, *J. Appl. Phys.* 42, Growth and characterization of liquid-phase epitaxial $InAs_xP_{1-x}$, pp. 3201-3204, 1971.
- (10) K. Nakajima, A. Yamaguchi, K. Akita and T. Kotani, Composition dependence of the band gaps of $In_{1-x}Ga_xAs_{1-y}P_y$ quaternary solid lattices matched to InP substrates, *J. Appl. Phys. Lett.* 49, pp. 5944-5950, 1978.
- (11) H. C. Casey, Jr and M. B. Panish, *Heterostructure Lasers, Part B*, Academic, New York, 1978.
- (12) P. F. Fewster and N. L. Andrew, Determining the lattice relaxation in semiconductor layer systems by x-ray diffraction, *J. Appl. Phys.* 74, pp. 3121-3125, 1993.
- (13) M. Wada, M. Seko, K. Sakakibara and Y. Sekiguchi, Zn diffusion into InP using dimethylzinc as Zn source, *Jpn. J. Appl. Phys.* 28, pp. L1700-1703, 1989.
- (14) M. Wada, K. Sakakibara, T. Umezawa, S. Nakajima, S. Araki, T. Kudou and T. Ueda, Diffusion of zinc in InP, InAsP and InGaAs by the metal-organic vapor-phase diffusion technique,

in *Defect and Diffusion Forum* Vol. 183-185, D. J. Fisher ed., Trans Tech Publications, Zürich, 2000, pp. 153-162.

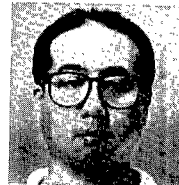
- (15) Z. F. Paska, D. Haga, and B. Willén, Highly doped p^+ regions by zinc diffusion utilizing metalorganic vapor-phase epitaxy, *Appl. Phys. Lett.* 60, pp. 1594-1596, 1992.

Morio Wada (Non-member) He received the B.S. and M.S. degrees in physics from the Science University of Tokyo in 1978 and 1980, respectively. In 1980 he joined the R&D Center, Yokogawa Electric Corporation. From 1987 to 1991 he worked in the Central Research laboratory, Optical Measurement



Technology Development Corporation, Tokyo. From 1991 to 2001, he was with the Optoelectronics Laboratory, R&D Center, Yokogawa Electric Corporation. He is currently the manager of the Optoelectronics Device Group, R&D Development Project Center, Yokogawa Electric Corporation. He is a member of Japan Society of Applied Physics and Physical Society of Japan.

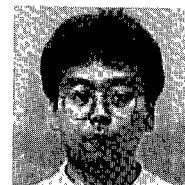
Shoujiro Araki (Non-member) He received the B.S. degree in physics from the Nihon University, Tokyo, in 1986. He joined the R&D Center, Yokogawa Electric Corporation in 1996, where he was engaged in research and development of MOVPE technologies for advanced photodetectors application.



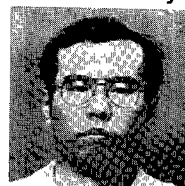
Kudou Takahiro (Non-member) He received the B.S. degree in physics in 1988 from the Science University of Tokyo. He joined the R&D Center, Yokogawa Electric Corporation in 1997, where he was engaged in research and development of MOVPE technologies for advanced photodetectors application. He is a member of several Japanese scientific societies.



Toshimasa Umezawa (Non-member) He received the M.S. degree in electrical engineering from Nagaoka University of Technology in 1987. In 1994 he received the Ph.D. degree in electrical engineering from Tokyo University. He is currently a member of the Optoelectronics Device Group, R&D Development Project Center, Yokogawa Electric Corporation, Tokyo. He is a member of Japan Society of Applied Physics.



Shinichi Nakajima (Non-member) He was born in Tokyo, Japan, in 1963. He received the M.S. degree in physics from the University of Tokyo, Japan, in 1987. In 1987 he joined Yokogawa Electric Corporation, where is currently working for the research and development of semiconductor-based optical devices. He is a member of Japan Society of Applied Physics.



Toshitsugu Ueda (Member) He was born in Nara, Japan, on October 4, 1945. He received the B.E. and M.E. degrees in electrical engineering from Shinshu University, Nagano, Japan, in 1969 and 1971, respectively. He received Ph.D. degree from Tokyo Institute of Technology in 1988. Since joining Yokogawa Electric Corporation in 1971, he has been engaged in developing low noise amplifiers, mechanical resonators, micro machining technologies and sensors using above mentioned technologies for temperature, pressure and displacement. Now he is a general manager of Corporate R&D department. He received Awards from Society of Instrument and Control Engineers of Japan in 1987 and 1994, and Awards from Japan Institute Invention and Innovation in 1985 and 1987. Dr. Ueda is a member of the Institute of Electrical Engineers of Japan, and Society of Instrument and Control Engineers of Japan.

